

Supplementary Information for:

Computational Characterization of the Selective Inhibition of Human Norepinephrine and Serotonin Transporters by Escitalopram Scaffold

Guoxun Zheng^{†,§}, Fengyuan Yang^{†,§}, Tingting Fu^{†,§}, Gao Tu^{†,§}, Yuzong Chen[‡], Xiaojun Yao^l, Weiwei Xue^{*,§} and Feng Zhu^{*,†,§}

[†] College of Pharmaceutical Sciences, Zhejiang University, Hangzhou 310058, China

[§] School of Pharmaceutical Sciences and Collaborative Innovation Center for Brain Science, Chongqing University, Chongqing 401331, China

[‡] Bioinformatics and Drug Design Group, Department of Pharmacy, National University of Singapore, Singapore 117543, Singapore

^l State Key Laboratory of Applied Organic Chemistry and Department of Chemistry, Lanzhou University, Lanzhou 730000, China

Corresponding Author

*Mailing address: College of Pharmaceutical Sciences, Zhejiang University, Hangzhou 310058, China. E-mail: zhufeng@zju.edu.cn and prof.zhufeng@gmail.com. Phone: +86-(0)571-8820-8444.

*Mailing address: School of Pharmaceutical Sciences, Chongqing University, Chongqing 401331, China. E-mail: xueww@cqu.edu.cn. Phone: +86-(0)23-65678468.

Supplementary Methods

MM/3D-RISM Calculation

The 3D-RISM calculations have been carried out via two steps. In the first step, bulk solvent (containing water and salt ions) properties has been estimated in one dimension with the aid of 1D-RISM based on the dielectrically consistent RISM (DRISM) theory¹. This gives the bulk solvent site-site pair correlation and produces the intramolecular matrix in reciprocal space, $\chi^{vv}(\mathbf{k})$. In the second step, with the results from 1D-RISM, solute-solvent correlation function will be subsequently calculated via 3D-RISM method²⁻⁴. In this work, 3D-RISM calculations have been performed using *rism1d* and *rism3d.snglpnt* routine implemented within *AmberTools 16*. The Kovalenko-Hirata (KH) closure⁵ has been applicable to the mixture liquid and utilized for the RISM calculations. For solvent calculation, TIP3P water model⁶ and *Joung-Cheatham LJ* parameters⁷ are adopted for Na⁺ and Cl⁻ (0.15 M NaCl concentration). The temperature is set to 298 K, and the dielectric constant of bulk water is set as 78.497. The non-polar part of solvation is computed by solving the Ornstein-Zernike (OZ) integral equation (thermo = 'gf') via averaging out the orientation degrees of the freedom of solvent molecules, keeping the orientation of the solute macromolecule described at the three-dimensional level. It is to be noted that the chemical potential calculated with the DRISM method is approximate⁸. Considering MM/3D-RISM calculation is computationally demanding, only 100 snapshots sampled from the last 100 ns trajectories are utilized for the calculation of binding free energies. Considering that the MM/3D-RISM method was more computationally demanding, only 100 snapshots from the last 100 ns trajectory of simulation were sampled to calculate the binding free energy. The energy was computed via the equation for each frame:

$$\Delta G_{\text{calc}} = \Delta E_{\text{MM}} + \Delta G_{\text{solvation}} \quad (2)$$

In Equation (2), $\Delta E_{\text{MM}} = \Delta E_{\text{vdW}} + \Delta E_{\text{EEL}}$ and $\Delta G_{\text{solvation}} = \Delta G_{\text{pol}} + \Delta G_{\text{apol}}$. ΔE_{MM} was the change in the gas-phase interaction energy on ligand binding. ΔE_{vdW} and ΔE_{EEL} were the change in van der Waals interactions and electrostatics energy on ligand binding, respectively. ΔG_{pol} and ΔG_{apol} were the change in polar and non-polar part of solvation free energy as a result of ligand binding to the protein.

Supplementary Tables

Table S1. The calculated and experimental binding free energies of six studied complexes (ΔG is in kcal/mol and K_i is in nM).

Complexes	Calculated values						Experimental values		
	ΔE_{ele}	ΔE_{vdW}	ΔG_{pol}	ΔG_{apol}	$\Delta G_{\text{MM/GBSA}}^a$	$\Delta \Delta G_{\text{MM/GBSA}}^b$	ΔG_{exp}^c	$\Delta \Delta G_{\text{exp}}^b$	K_i^d
Talopram-hNET	-24.52 ± 0.10	-52.13 ± 0.11	25.48 ± 0.09	-5.82 ± 0.01	-56.99 ± 0.11	-6.90	-10.64	-4.74	16
Escitalopram-hSERT	-25.47 ± 0.13	-50.07 ± 0.11	27.51 ± 0.11	-5.47 ± 0.00	-56.32 ± 0.11	-6.23	-10.48	-4.58	21
Ligand10-hNET	-29.89 ± 0.14	-46.18 ± 0.13	31.95 ± 0.13	-5.97 ± 0.01	-53.51 ± 0.11	-3.42	-9.05	-3.15	233
Ligand10-hSERT	-28.46 ± 0.21	-56.01 ± 0.11	34.28 ± 0.17	-6.12 ± 0.01	-53.29 ± 0.12	-3.20	-8.55	-2.65	542
Talopram-hSERT	-23.86 ± 0.21	-51.59 ± 0.11	27.63 ± 0.16	-5.46 ± 0.01	-51.40 ± 0.11	-1.31	-6.21	-0.31	28108
Escitalopram-hNET	-24.73 ± 0.17	-50.47 ± 0.11	29.49 ± 0.15	-5.70 ± 0.01	-50.09 ± 0.10	0.00	-5.90	0.00	47140

^a Calculated MM/GBSA binding free energies in this work.

^b $\Delta \Delta G$ is defined as the change of binding free energy (ΔG) using the system of escitalopram-hNET as a reference.

^c Estimated binding free energy based on experimental K_i values by $\Delta G_{\text{exp}} = RT \ln(K_i)$.

^d Experimental K_i values.

Table S2. The calculated entropic contributions of six studied complexes (unit is in kcal/mol).

Complexes	Normal mode			
	$-T\Delta S^a$	$\Delta G_{\text{trans.}}$	ΔG_{rota}	ΔG_{vibra}
Talopram-hNET	21.18 ± 2.19	-12.79 ± 0.00	-10.26 ± 0.00	1.87 ± 2.54
Escitalopram-hSERT	21.54 ± 2.20	-12.19 ± 0.00	-10.60 ± 0.00	1.93 ± 2.21
Ligand 10 -hNET	21.01 ± 3.83	-12.76 ± 0.00	-10.26 ± 0.00	2.01 ± 2.12
Ligand 10 -hSERT	21.28 ± 2.46	-12.76 ± 0.00	-10.28 ± 0.00	1.24 ± 2.46
Talopram-hSERT	21.31 ± 2.02	-12.79 ± 0.00	-10.24 ± 0.00	1.72 ± 2.02
Escitalopram-hNET	20.23 ± 2.33	-12.88 ± 0.00	-10.51 ± 0.00	3.16 ± 2.31

^a The enthalpy contributions ($-T\Delta S$) were calculated via normal mode analysis based on 10 frames extracted from the last 100 ns trajectory.

Table S3. The calculated binding free energies of six systems on different windows (ΔG is in kcal/mol).

Complexes	$\Delta G_{\text{MM/GBSA}}^a$			
	100-200 ns	200-300 ns	300-400 ns	400-500 ns
Talopram-hNET	-56.14	-55.98	-56.66	-56.99
Escitalopram-hSERT	-56.41	-56.54	-56.27	-56.32
Ligand 10 -hNET	-52.49	-52.93	-53.17	-53.51
Ligand 10 -hSERT	-53.90	-53.58	-54.25	-53.29
Talopram-hSERT	-52.24	-51.68	-51.69	-51.40
Escitalopram-hNET	-52.52	-50.33	-51.50	-50.09

^a Calculated MM/GBSA binding free energies in this work, ignoring the entropy contributions.

Table S4. The energies of thermodynamic integration for each step in the mutations of ligand10 to escitalopram and talopram (ΔG is in kcal/mol).

Systems	Mutations	ΔG^a			ΔG_{Sum}^b	$\Delta \Delta G_{\text{TI}}^c$	$\text{FC}_{K_i}^d$	$\Delta \Delta G_{\text{exp}}^e$	
		decharge	vdw-bonded	recharge					
hNET	Ligand10 \rightarrow Escitalopram	ligands	-4.27	1.47	-9.85	-12.65	-3.28	202	-3.15
		complex	-3.27	-0.90	-11.76	-15.93			
	Ligand10 \rightarrow Talopram	ligands	-6.24	0.87	-6.88	-12.25	1.03	0.07	1.59
		complex	-3.28	1.59	-9.53	-11.22			
hSERT	Ligand10 \rightarrow Escitalopram	ligands	-5.94	-1.26	-14.72	-21.92	2.03	0.04	1.93
		complex	-3.97	-0.94	-14.98	-19.89			
	Ligand10 \rightarrow Talopram	ligands	-6.05	1.48	-14.76	-19.33	-1.57	52	-2.34
		complex	-4.98	-1.56	-14.36	-20.90			

^a The energy calculated by thermodynamic integration for decharge, vdw-bonded and recharge based on λ ranging from 0.0 to 1.0.

^b ΔG Sum is the sum of the $\Delta G_{\text{decharge}}$, $\Delta G_{\text{vdw-bonded}}$, and $\Delta G_{\text{recharge}}$

^c $\Delta \Delta G$ is computed via the equation, $\Delta \Delta G = \Delta G_{\text{com .Sum}} - \Delta G_{\text{lig .Sum}}$

^d FC_{K_i} indicates the fold change of two ligands based on their K_i .

^e $\Delta \Delta G_{\text{exp}}$ is the experimental binding free energy based on experimental K_i values by $\Delta \Delta G_{\text{exp}} = -RT \ln(\text{FC}_{K_i})$.

Table S5. The calculated binding free energies of six systems via MM/3D-RISM (ΔG is in kcal/mol).

Complexes	Experimental Values		MM/3D-RISM					
	K_i^a	ΔG_{exp}^b	ΔG_{total}	ΔE_{vdW}	ΔE_{EEL}	ΔG_{ERISM}	ΔG_{gas}	ΔG_{solv}
Talopram-hNET	16	-10.64	-75.27 ± 2.22	-47.72 ± 0.44	-51.87 ± 2.80	24.31 ± 0.98	-99.59 ± 2.75	24.32 ± 0.98
Escitalopram-hSERT	21	-10.48	-92.98 ± 0.97	-55.63 ± 0.64	-42.91 ± 1.83	5.56 ± 1.11	-98.54 ± 1.63	5.56 ± 1.11
Ligand10-hNET	233	-9.05	-80.81 ± 1.95	-45.95 ± 0.88	-67.96 ± 3.27	33.10 ± 2.06	-113.91 ± 3.07	33.10 ± 2.06
Ligand10-hSERT	542	-8.55	-86.45 ± 1.11	-51.22 ± 0.78	-48.49 ± 1.95	13.26 ± 1.45	-99.71 ± 1.71	13.26 ± 1.45
Talopram-hSERT	28108	-6.21	-99.80 ± 1.91	-54.00 ± 1.02	-53.89 ± 1.59	8.09 ± 1.06	-107.89 ± 1.93	8.09 ± 1.06
Escitalopram-hNET	47140	-5.90	-77.11 ± 1.48	-47.68 ± 0.49	-61.12 ± 2.09	31.69 ± 0.85	-108.80 ± 1.95	31.69 ± 0.85

^a Experimental K_i values.

^b ΔG_{exp} is the experimental binding free energy based on experimental K_i values by $\Delta G_{\text{exp}} = RT \ln(K_i)$.

Table S6. Interaction fingerprints between 3 ligands and 13 residues in hNET and the interaction types.

Residues	Fingerprints ^a	Interaction Type
F72	1000000	Hydrophobic
A73	1000000	Hydrophobic
D75	1000000	Hydrophobic + H-bond (ligand donor) + Ionic (ligand. charged +)
A145	1000000	Hydrophobic
V148	1000000	Hydrophobic
Y151	1000000	Hydrophobic
Y152	1100000	Hydrophobic + Aromatic (face-to-face)
F323	1000000	Hydrophobic
S419	1000000	Hydrophobic
S420	1000000	Hydrophobic
M424	1000000	Hydrophobic
A477	1000000	Hydrophobic
I481	1000000	Hydrophobic

^a **1st** position: Hydrophobic; **2nd** position: Aromatic (face-to-face); **3rd** position: Aromatic (edge-to-face); **4th** position: H-bond (protein donor); **5th** position: H-bond (ligand donor); **6th** position: Ionic (protein donor); **7th** position: Ionic (ligand donor); 0: No; 1: Yes.

Table S7. Interaction fingerprints between 3 ligands and 15 residues in hSERT and the interaction types.

Residues	Fingerprints ^a	Interaction Type
Y95	1000000	Hydrophobic
A96	1000000	Hydrophobic
D98	1000000	Hydrophobic + H-bond (ligand donor) + Ionic (ligand. charged +)
A169	1000000	Hydrophobic
I172	1000000	Hydrophobic
A173	1000000	Hydrophobic
Y175	1100000	Hydrophobic + Aromatic (face-to-face)
Y176	1010000	Hydrophobic + Aromatic (edge-to-face)
F335	1000000	Hydrophobic
F341	1000000	Hydrophobic
S438	1000000	Hydrophobic
T439	1000000	Hydrophobic
L443	1000000	Hydrophobic
T497	1000000	Hydrophobic
V501	1000000	Hydrophobic

^a **1st** position: Hydrophobic; **2nd** position: Aromatic (face-to-face); **3rd** position: Aromatic (edge-to-face); **4th** position: H-bond (protein donor); **5th** position: H-bond (ligand donor); **6th** position: Ionic (protein donor); **7th** position: Ionic (ligand donor); 0: No; 1: Yes.

Table S8. The binding free energy contributions from the backbones (b.b.) and side chains (s.c.) of the residues around the P1 ~ P4 of ligands among the 3 systems including escitalopram-hNET, ligand10-hNET and talopram-hNET (ΔG is in kcal/mol).

P1-P4	Systems	Escitalopram-hSERT			Ligand10-hSERT			Talopram-hSERT		
	Residues	$\Delta G_{s.c.}^a$	$\Delta G_{b.b.}^b$	ΔG_{total}^c	$\Delta G_{s.c.}$	$\Delta G_{b.b.}$	ΔG_{total}	$\Delta G_{s.c.}$	$\Delta G_{b.b.}$	ΔG_{total}
P1-diMet	F316	-0.05	-0.15	-0.20	-0.07	-0.06	-0.13	-0.52	-0.23	-0.75
	F317	-0.81	-0.34	-1.15	-0.53	-0.75	-1.28	-0.33	-0.23	-0.56
	A477	-0.06	-0.04	-0.10	-0.02	-0.04	-0.06	-0.53	-0.26	-0.79
	I481	-0.82	-0.02	-0.84	-0.08	-0.01	-0.09	-0.71	-0.03	-0.74
	G320	-0.36	-0.54	-0.90	-0.32	-0.39	-0.70	-0.39	-0.41	-0.81
	F323	-1.19	-0.01	-1.21	-1.77	-0.04	-1.81	-1.10	-0.03	-1.14
	SUM	-3.29	-1.10	-4.40	-2.79	-1.29	-4.07	-3.58	-1.19	-4.79
P2-CN	V148	-1.88	-0.35	-2.23	-2.03	-0.42	-2.46	-2.17	-0.50	-2.67
	Y151	-0.41	-0.05	-0.47	-0.45	-0.06	-0.51	-0.57	-0.10	-0.66
	F317	-0.81	-0.34	-1.15	-0.53	-0.75	-1.28	-0.33	-0.23	-0.56
	A477	-0.06	-0.04	-0.10	-0.02	-0.04	-0.06	-0.53	-0.26	-0.79
	I481	-0.82	-0.02	-0.84	-0.08	-0.01	-0.09	-0.71	-0.03	-0.74
	SUM	-3.98	-0.80	-4.79	-3.11	-1.28	-4.40	-4.31	-1.12	-5.42
	P3-F	A145	-0.31	-0.32	-0.62	-0.30	-0.27	-0.58	-0.25	-0.20
V148		-1.88	-0.35	-2.23	-2.03	-0.42	-2.46	-2.17	-0.50	-2.67
G149		-0.16	-0.37	-0.53	-0.17	-0.46	-0.63	-0.20	-0.38	-0.58
S420		-0.63	-0.66	-1.29	-0.46	-0.51	-0.98	-0.24	-0.39	-0.62
G423		-0.30	-0.63	-0.92	-0.38	-0.84	-1.22	-0.24	-0.50	-0.74
M424		-0.40	-0.23	-0.63	-0.37	-0.27	-0.65	-0.05	-0.08	-0.13
SUM		-3.68	-2.56	-6.22	-3.71	-2.77	-6.52	-3.15	-2.05	-5.19
P4-Met	F72	-2.75	-0.21	-2.96	-3.26	-1.20	-4.47	-2.30	-1.57	-3.87
	A73	-0.18	-0.40	-0.58	-0.27	-0.67	-0.94	-0.38	-1.06	-1.45
	D75	-2.34	-0.15	-2.49	-3.62	-0.28	-3.90	-3.31	-0.33	-3.64
	S318	-0.34	-0.65	-0.99	-0.20	-0.62	-0.82	-0.04	-0.31	-0.35
	G320	-0.36	-0.54	-0.90	-0.32	-0.39	-0.70	-0.39	-0.41	-0.81
	S419	-0.62	-0.14	-0.76	-0.78	-0.41	-1.18	-1.24	-0.26	-1.50
	SUM	-6.59	-2.09	-8.68	-8.45	-3.57	-12.01	-7.66	-3.94	-11.62
Total			-24.09			-27.00			-27.02	

^a $\Delta G_{s.c.}$ indicates the energy contribution of the side chains to the ligands binding to hNET.

^b $\Delta G_{b.b.}$ refers to the energy contribution of the backbones to the ligands binding to hNET.

^c ΔG_{total} means the total energy contribution of side chains and backbones to ligands binding to hNET.

Table S9. The binding free energy contributions from the backbones (b.b.) and side chains (s.c.) of the residues around the P1 ~ P4 of ligands among the 3 systems including escitalopram-hSERT, ligand10-hSERT and talopram-hSERT (ΔG is in kcal/mol).

P1-P4	Systems	Escitalopram-hSERT			Ligand10-hSERT			Talopram-hSERT		
	Residues	$\Delta G_{s.c.}^a$	$\Delta G_{b.b.}^b$	ΔG_{total}^c	$\Delta G_{s.c.}$	$\Delta G_{b.b.}$	ΔG_{total}	$\Delta G_{s.c.}$	$\Delta G_{b.b.}$	ΔG_{total}
P1-diMet	F335	-0.60	-0.16	-0.77	-0.53	-0.20	-0.73	-0.64	-0.51	-1.15
	G338	-0.32	-0.53	-0.85	-0.32	-0.60	-0.92	-0.39	-0.50	-0.89
	F341	-1.25	0.01	-1.24	-1.34	-0.04	-1.38	-1.24	0.00	-1.24
	SUM	-2.17	-0.68	-2.86	-2.19	-0.84	-3.03	-2.27	-1.01	-3.28
P2-CN	I172	-2.80	-0.41	-3.21	-2.64	-0.38	-3.02	-2.58	-0.33	-2.91
	Y175	-0.38	-0.06	-0.44	-0.17	-0.08	-0.25	-0.22	-0.07	-0.29
	F335	-0.60	-0.16	-0.77	-0.53	-0.20	-0.73	--- ^d	--- ^d	--- ^d
	T497	-0.22	-0.32	-0.54	-0.38	-0.05	-0.43	-0.51	-0.08	-0.59
	V501	-0.73	-0.04	-0.77	-0.37	-0.03	-0.39	-0.72	0.02	-0.69
	SUM	-4.73	-0.99	-5.73	-4.09	-0.73	-4.82	-4.03	-0.46	-4.48
	SUM	-4.73	-0.99	-5.73	-4.09	-0.73	-4.82	-4.03	-0.46	-4.48
P3-F	A169	-0.18	-0.19	-0.37	-0.28	-0.20	-0.48	-0.14	-0.14	-0.28
	A173	-0.25	-0.32	-0.56	-0.18	-0.27	-0.46	-0.28	-0.22	-0.49
	T439	-0.72	-0.47	-1.19	-0.50	-0.46	-0.96	-0.38	-0.40	-0.77
	G442	-0.38	-0.95	-1.33	-0.36	-1.00	-1.36	-0.25	-0.49	-0.73
	L443	-0.61	-0.22	-0.82	-0.48	-0.17	-0.65	-0.20	-0.10	-0.30
	SUM	-2.14	-2.15	-4.27	-1.80	-2.10	-3.91	-1.25	-1.35	-2.57
P4-Met	Y95	-3.58	-1.40	-4.97	-3.01	-1.37	-4.39	-3.41	-1.16	-4.57
	A96	-0.35	-0.36	-0.70	-0.33	-1.24	-1.57	-0.26	-0.68	-0.95
	D98	-5.30	-0.24	-5.54	-4.00	-0.32	-4.33	-3.01	-0.20	-3.21
	S336	-0.32	-0.87	-1.18	-0.37	-0.80	-1.17	-0.34	-0.64	-0.98
	G338	-0.32	-0.53	-0.85	-0.32	-0.60	-0.92	-0.39	-0.50	-0.89
	S438	-0.74	-0.10	-0.85	-0.82	-0.12	-0.94	-0.54	-0.27	-0.81
	SUM	-10.61	-3.50	-14.09	-8.85	-4.45	-13.32	-7.95	-3.45	-11.41
Total			-26.95			-25.08			-21.74	

^a $\Delta G_{s.c.}$ indicates the energy contribution of the side chains to the ligands binding to hSERT.

^b $\Delta G_{b.b.}$ refers to the energy contribution of the backbones to the ligands binding to hSERT.

^c ΔG_{total} means the total energy contribution of side chains and backbones to ligands binding to hSERT.

^d NA. Due to the long distance between F335 and P2 of talopram.

Supplementary Figures

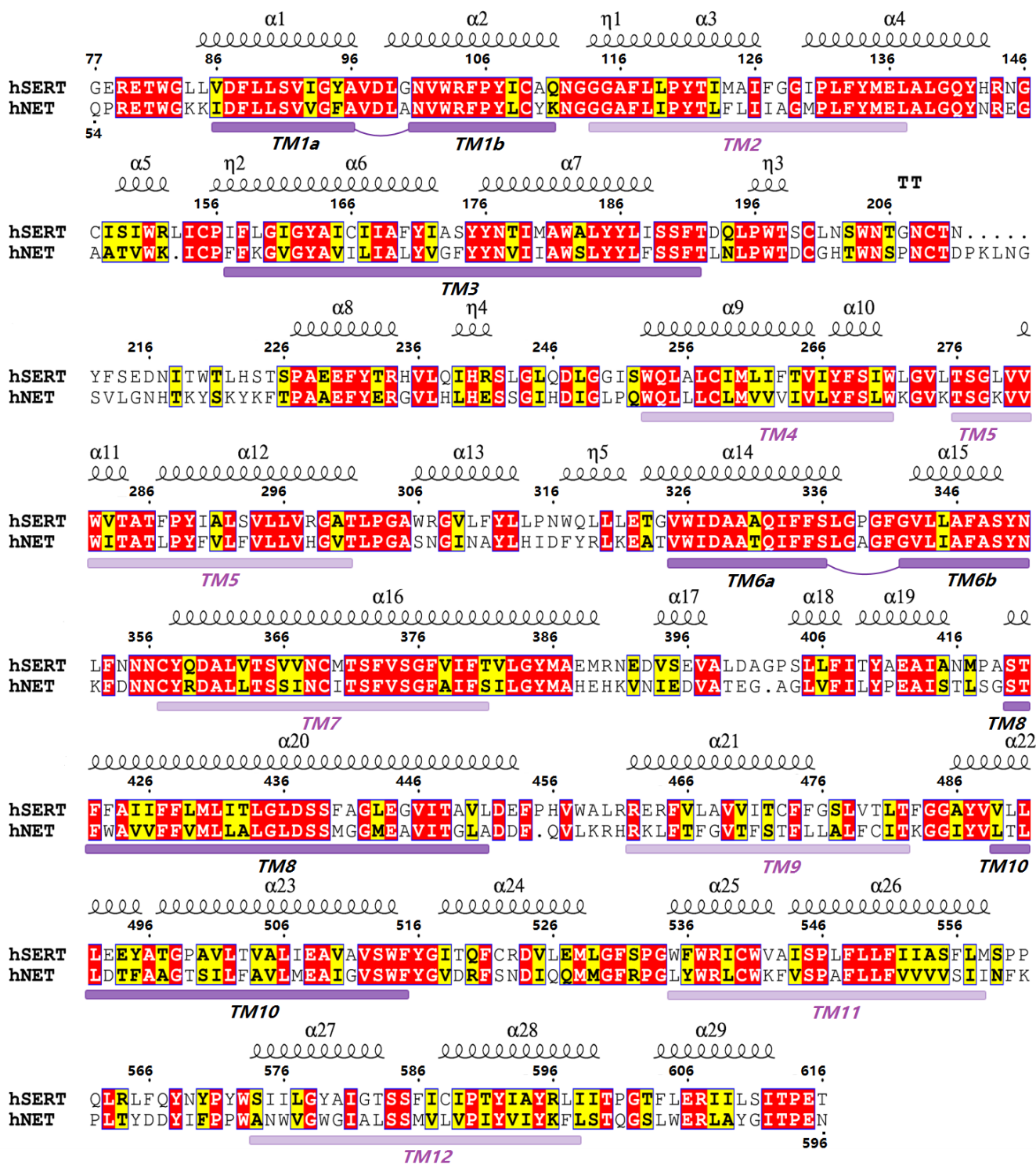
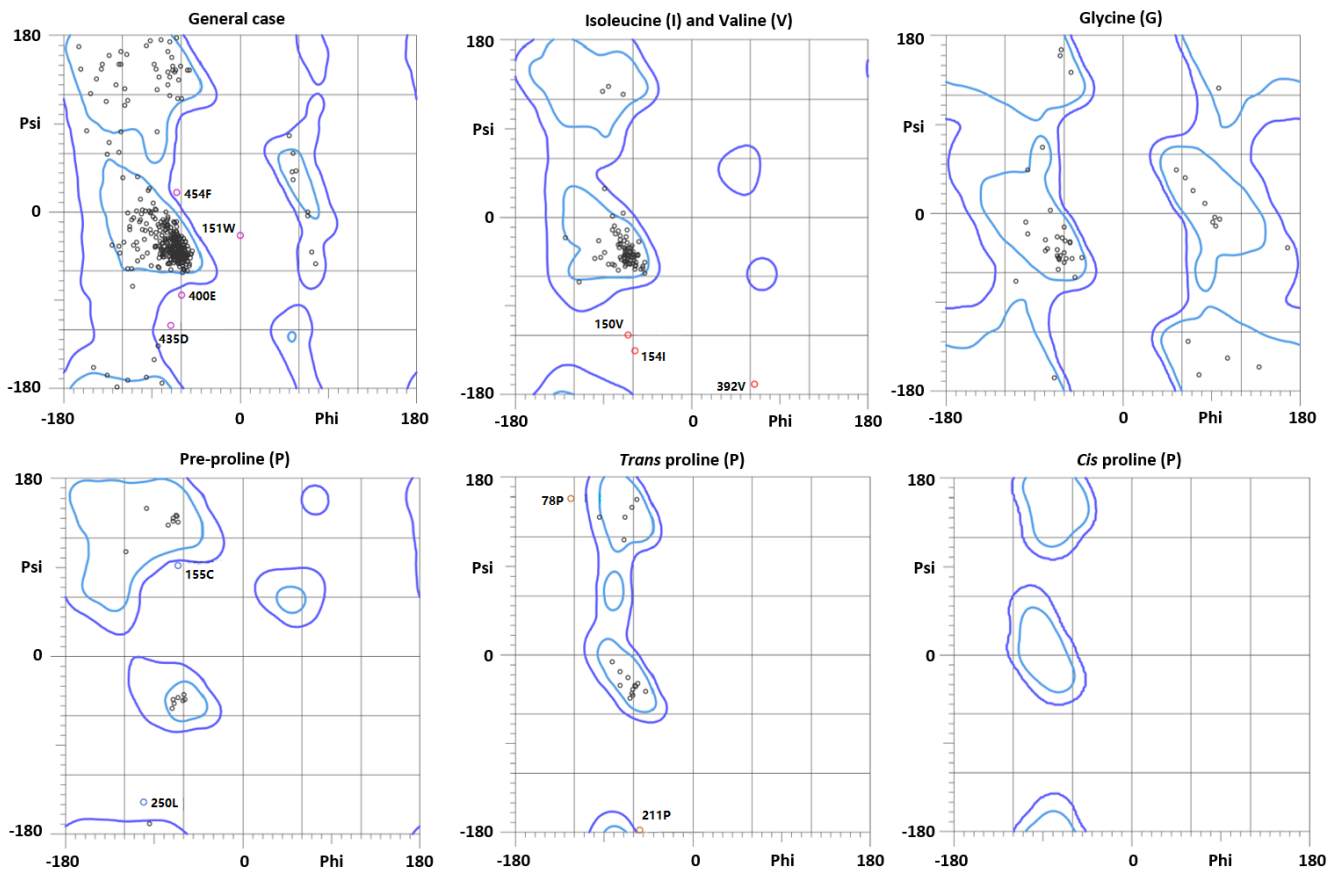


Figure S1. The visualization of sequence alignment result between target hNET (Entry code: P23975⁹, from Q54 to N596) and template hSERT (PDB entry: 5I71¹⁰, from G77 to T616) via *ESPrpt*¹¹. Sequence alignment was performed in *ClustalX*¹². The 12 transmembrane (TM1-12) domains were marked in purple or light purple color on sequence, and the TM1, 3, 6, 8 and 10 were stressed in purple color. The calculated sequence identity between hNET and hSERT was 54%. The residues colored in red and yellow represent fully identical and very similar, respectively.



- 93.1% (501/538) of all residues were in favored (98%) regions.
- 98.0% (527/538) of all residues were in allowed (>99.8%) regions
- There were 11 outliers (phi, psi): 78P (-124.4, 159.1), 150V (-65.6, -120.0), 151W (-0.8, -24.6), 154I (-58.1, -136.8), 155C (-66.7, 92.1), 211P (-54.6, -178.4), 250L (-101.6, -148.8), 392V (64.7, -170.2), 400E (-60.0, -85.2), 435D (-71.7, -116.6), 454F (-65.2, 20.6)

Figure S2. MolProbity Ramachandran analysis of the modeled hNET structure. 93.1% of all the residues were located in favored regions and 98.0% of all the residues were in allowed regions.

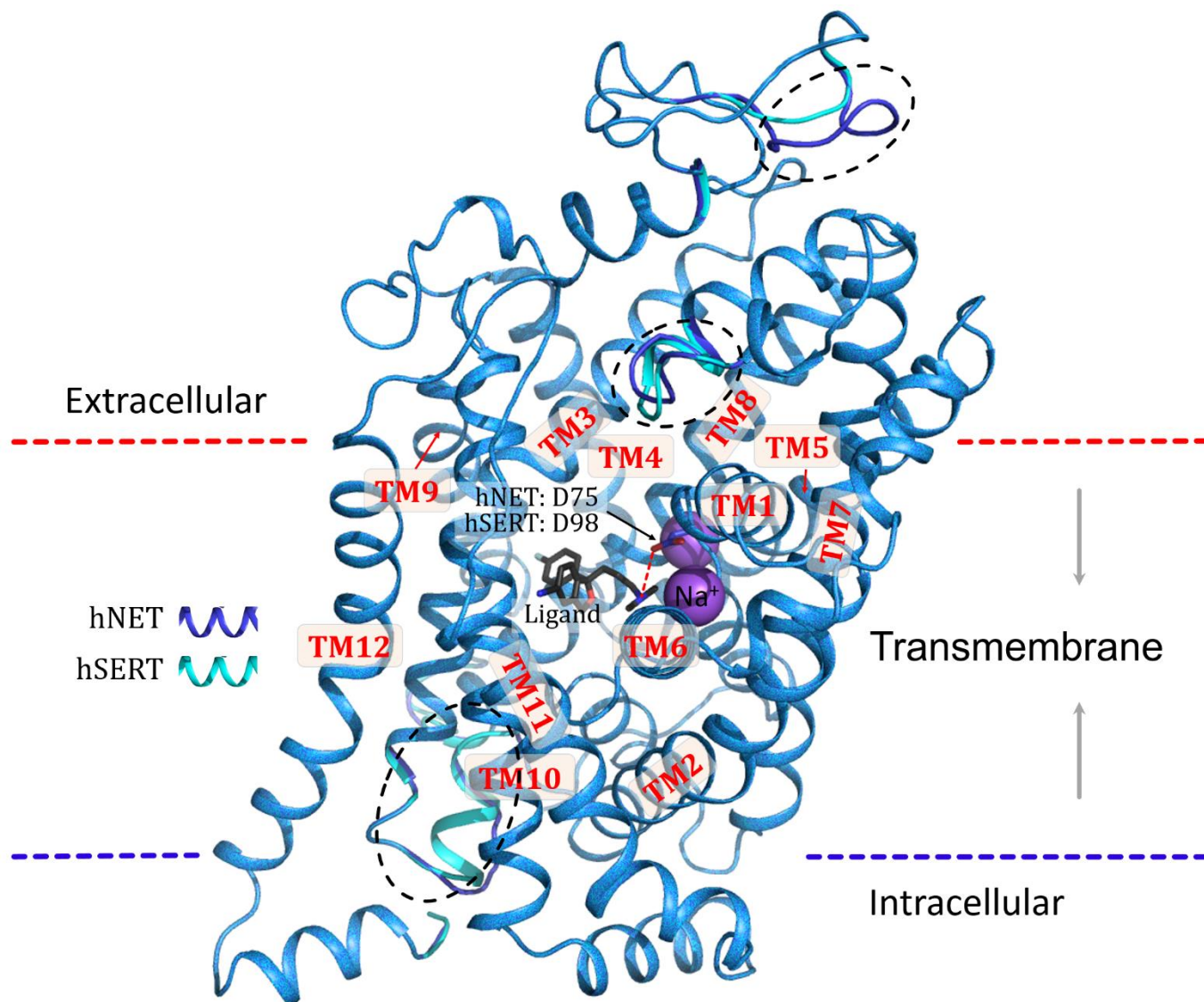


Figure S3. Structural superimposition of the modeled hNET (in blue cartoon) and the modified hSERT crystal structure (in cyan cartoon). Both hNET and hSERT covered the 12 transmembrane helices (TM1-12) domains, intracellular and extracellular loops. The three parts in red dashed boxes indicated the subtle displacements between hNET and hSERT.

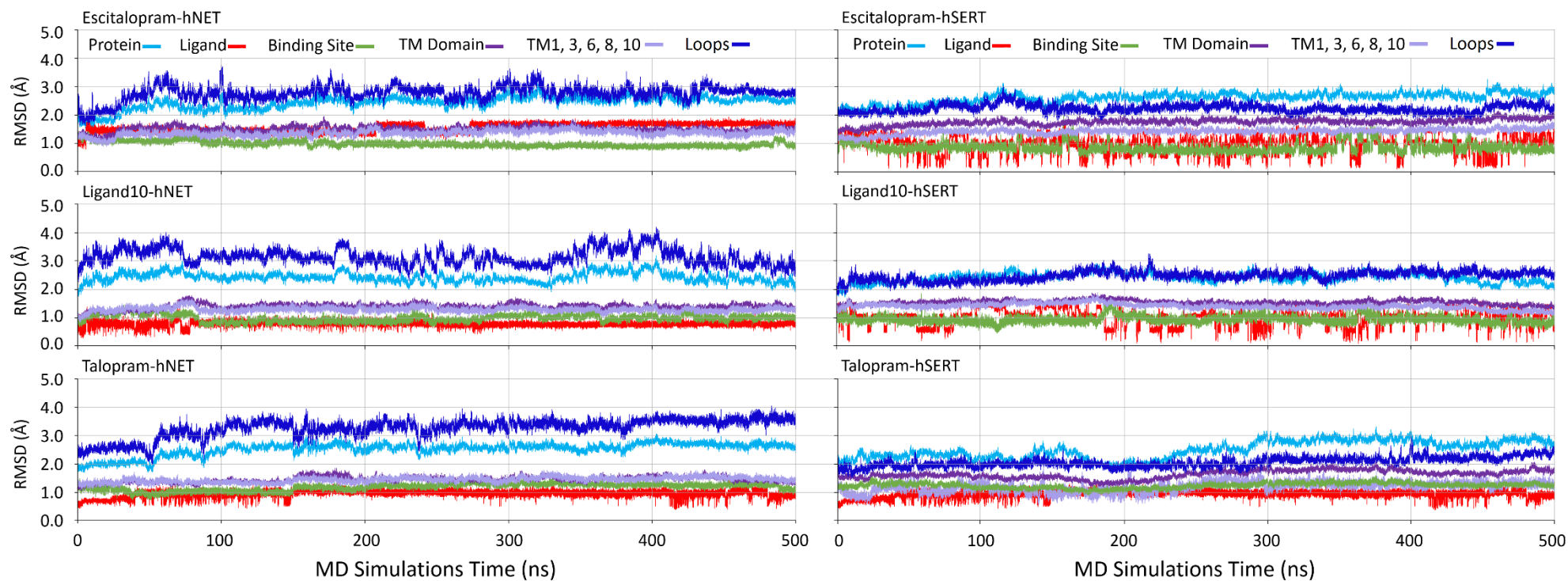


Figure S4. The RMSD values (Å) of protein (in cyan), ligand (in red), binding site (around ligands < 6.0 Å) (in green), transmembrane domains (TM1-12) (in purple), loop regions (in blue) and TM1, 3, 6, 8 and 10 (in light blue) of the six studied complexes against simulation time (ns) with respect to the corresponding initial structure.

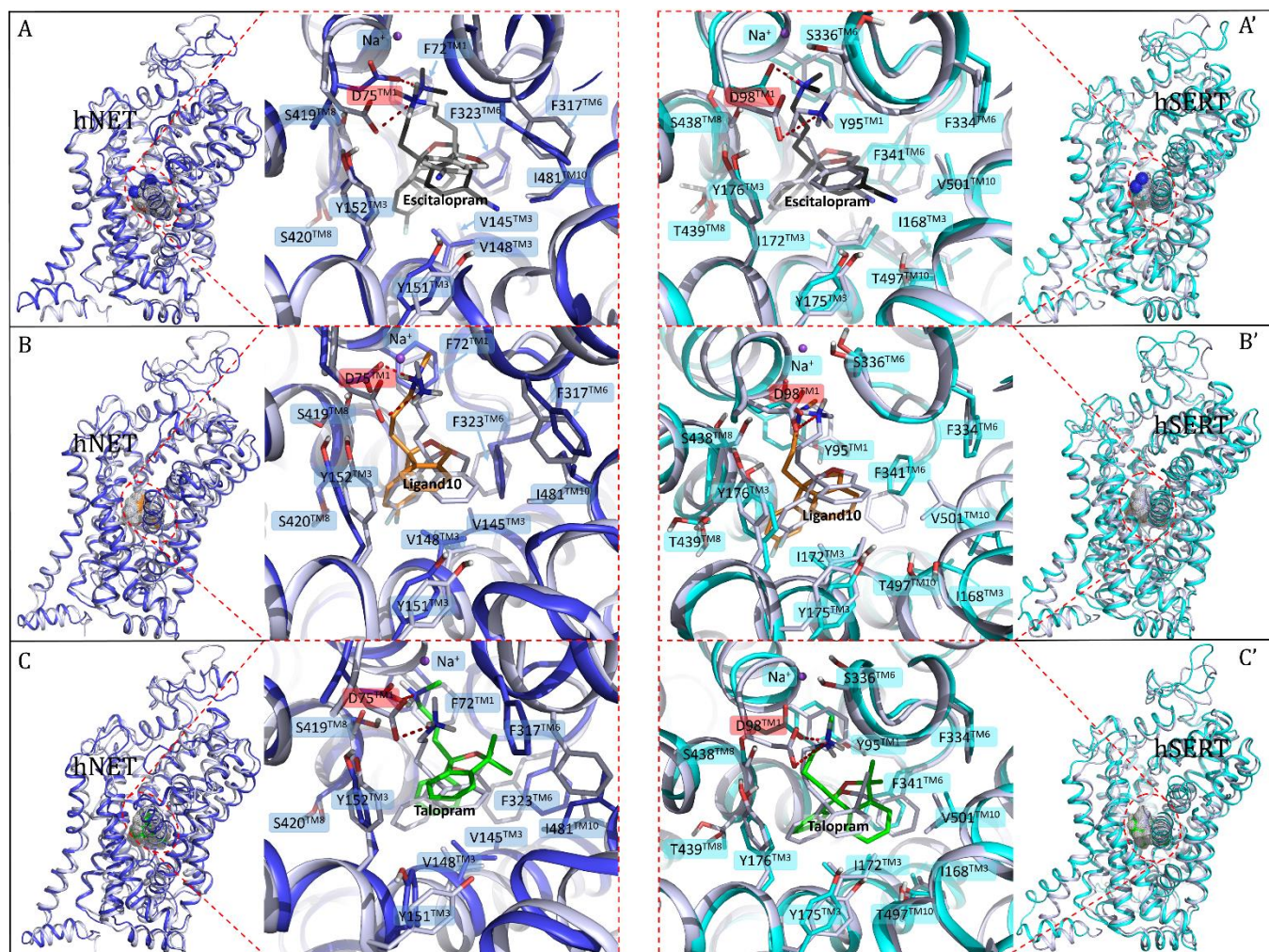


Figure S5. The superimposition of the representative snapshots and the initial poses of the 6 systems. A)-C) shown the comparison of the conformations of escitalopram, **10** and talopram binding to hNET and the conformations of proteins before (ligands in grey stick and hNET in grey cartoon) and after (escitalopram in dark stick, ligand10 in orange stick, talopram in green stick and hNET in blue cartoon) MD simulations. A')-C') shown the comparison of the conformations of escitalopram, ligand10 and talopram binding to hSERT and the conformations of proteins before (ligands in grey stick and hSERT in grey cartoon) and after (escitalopram in dark stick, ligand10 in orange stick, talopram in green stick and hNET in cyan cartoon) MD simulations. The binding sites of hNET and hSERT were marked by ligands in surface and circled by the dashed lines. The residue names and their transmembrane domains were labeled on the corresponding sites. The salt bridges between the residues (D75 in hNET and D98 in hSERT) and the positively charged amine groups were displayed in red dotted.

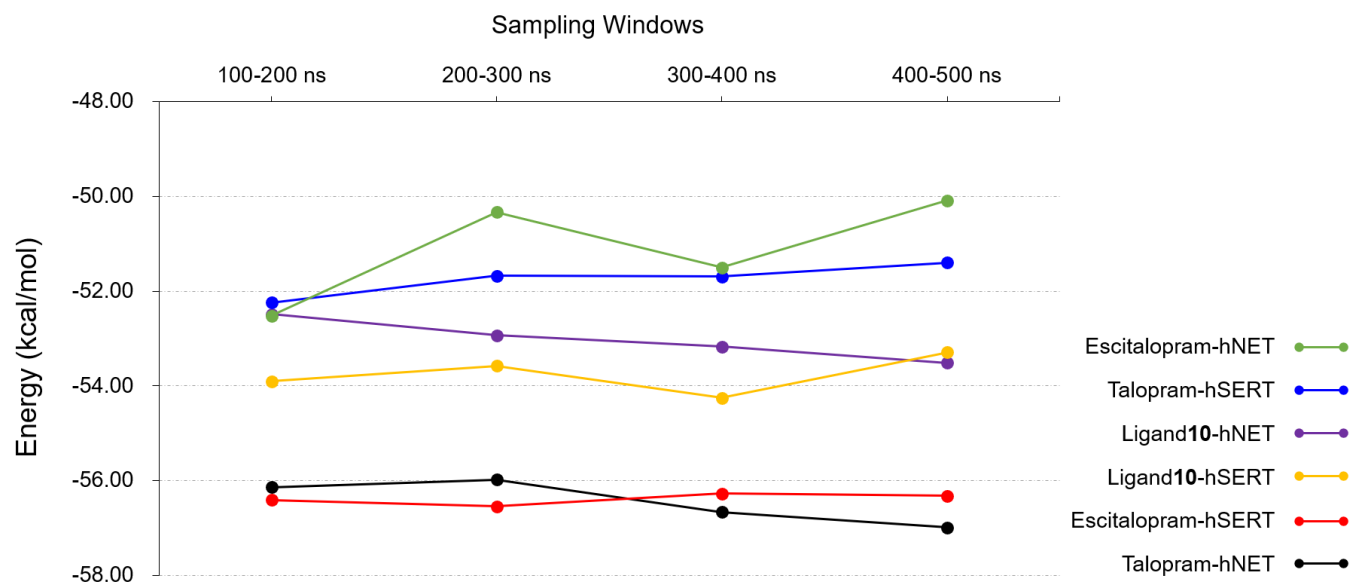


Figure S6. The binding free energies calculated based on different simulation windows (100 - 200 ns, 200 - 300 ns, 300 - 400 ns, and 400 - 500 ns, 1000 snapshots) during the whole 500 ns simulation.

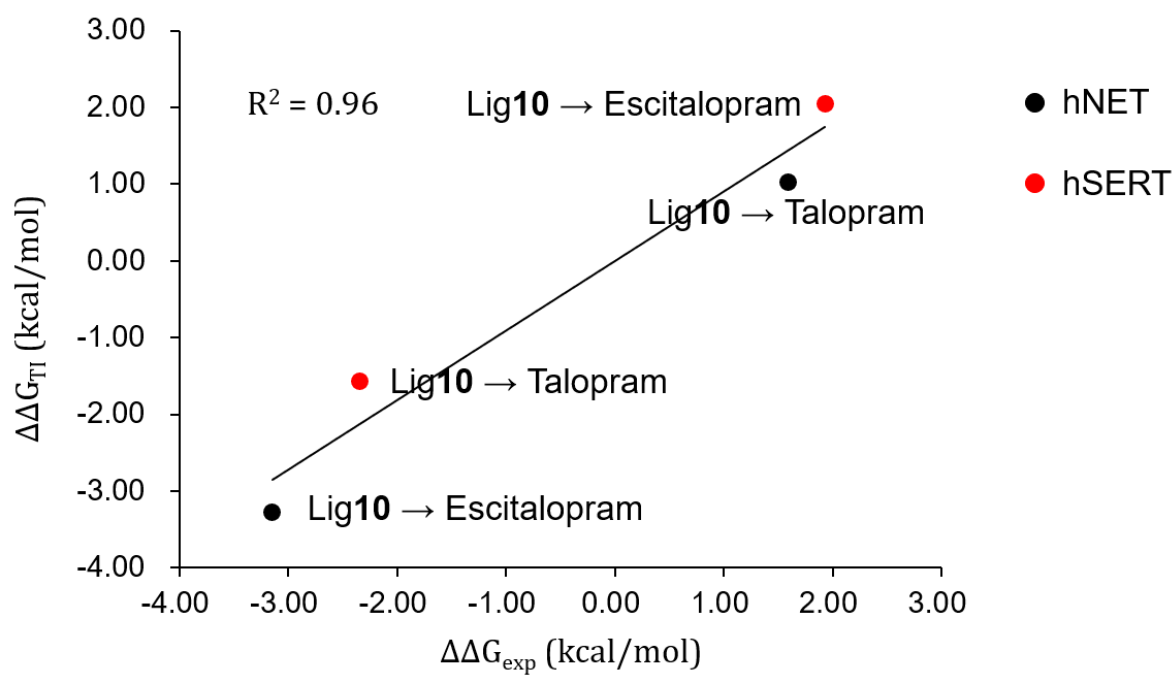


Figure S7. The correlation coefficient (R^2) between the calculated and experimental values ($\Delta\Delta G$) using TI method.

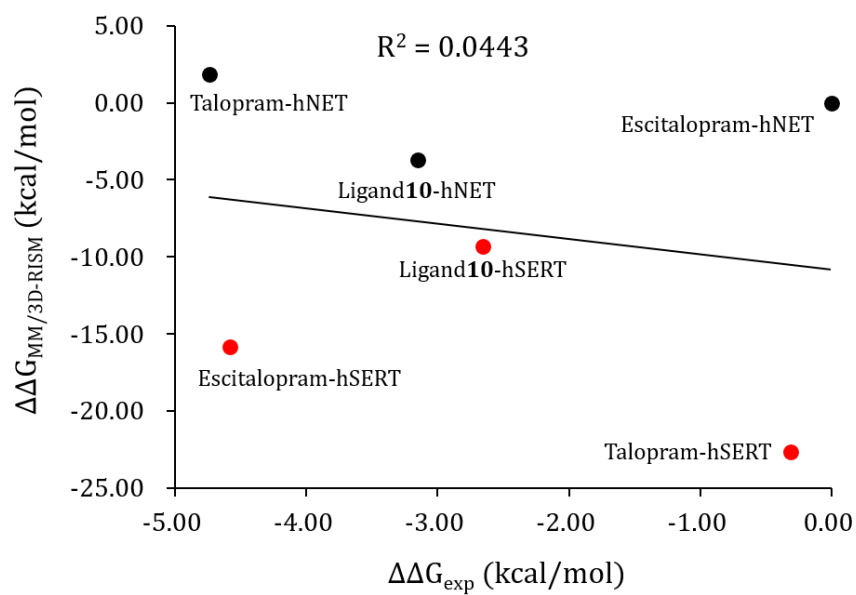


Figure S8. The correlation coefficient (R^2) between the difference of the calculated and experimental values ($\Delta\Delta G$) using MM/3D-RISM method.

References

- 1 T. Luchko; S. Gusarov; D. R. Roe; C. Simmerling; D. A. Case; J. Tuszynski; A. Kovalenko. Three-dimensional molecular theory of solvation coupled with molecular dynamics in Amber. *J Chem Theory Comput.* 2010, 6(3): 607-24
- 2 A. Kovalenko; F. Hirata. Three-dimensional density profiles of water in contact with a solute of arbitrary shape: A RISM approach. *Chemical Physics Letters.* 1998, 290(1-3): 237-44
- 3 M. Sugita; F. Hirata. Predicting the binding free energy of the inclusion process of 2-hydroxypropyl-beta-cyclodextrin and small molecules by means of the MM/3D-RISM method. *J Phys Condens Matter.* 2016, 28(38): 384002
- 4 P. Pandey; R. Srivastava; P. Bandyopadhyay. Comparison of molecular mechanics-Poisson-Boltzmann surface area (MM-PBSA) and molecular mechanics-three-dimensional reference interaction site model (MM-3D-RISM) method to calculate the binding free energy of protein-ligand complexes: Effect of metal ion and advance statistical test. *Chemical Physics Letters.* 2018, 69569-78
- 5 H. A. Yu; B. Roux; M. Karplus. Solvation Thermodynamics - an Approach from Analytic Temperature Derivatives. *Journal of Chemical Physics.* 1990, 92(8): 5020-32
- 6 W. L. Jorgensen; J. Chandrasekhar; J. D. Madura; R. W. Impey; M. L. Klein. Comparison of Simple Potential Functions for Simulating Liquid Water. *Journal of Chemical Physics.* 1983, 79(2): 926-35
- 7 I. S. Joung; T. E. Cheatham. Molecular Dynamics Simulations of the Dynamic and Energetic Properties of Alkali and Halide Ions Using Water-Model-Specific Ion Parameters. *Journal of Physical Chemistry B.* 2009, 113(40): 13279-90
- 8 I. S. Joung; T. Luchko; D. A. Case. Simple electrolyte solutions: comparison of DRISM and molecular dynamics results for alkali halide solutions. *Journal of Chemical Physics.* 2013, 138(4): 044103
- 9 T. Pacholczyk; R. D. Blakely; S. G. Amara. Expression cloning of a cocaine-and antidepressant-sensitive human noradrenaline transporter. *Nature.* 1991, 350(6316): 350-54
- 10 J. A. Coleman; E. M. Green; E. Gouaux. X-ray structures and mechanism of the human serotonin transporter. *Nature.* 2016, 532(7599): 334-39
- 11 X. Robert; P. Gouet. Deciphering key features in protein structures with the new ENDscript server. *Nucleic Acids Res.* 2014, 42(Web Server issue): W320-24
- 12 M. A. Larkin; G. Blackshields; N. P. Brown; R. Chenna; P. A. McGettigan; H. McWilliam; F. Valentin; I. M. Wallace; A. Wilm; R. Lopez; J. D. Thompson; T. J. Gibson; D. G. Higgins. Clustal W and Clustal X version 2.0. *Bioinformatics.* 2007, 23(21): 2947-48